# Photoluminescent layered Y/Er silicates

Mariya H. Kostova[a], Duarte Ananias[a,b], Luís D. Carlos[c,*], João Rocha[a,**]

[a] *Department of Chemistry, CICECO, University of Aveiro, 3810-193 Aveiro, Portugal*
[b] *Department of Biochemistry, University of Coimbra, 3001-401 Coimbra, Portugal*
[c] *Department of Physics, CICECO, University of Aveiro, 3810-193 Aveiro, Portugal*

Available online 13 April 2007

## Abstract

The synthesis of new layered rare-earth silicates $K_3[Y_{1-a}Er_aSi_3O_8(OH)_2]$ (AV-22 materials) has been reported. The photoluminescence properties of Y/Er-AV-22 and the material resulting from its thermal degradation, $K_3[Y_{1-a}Er_aSi_3O_9]$ (Y/Er-AV-23), have been studied and compared. Both materials have a similar chemical makeup and structures sharing analogous building blocks, hence providing a unique opportunity for rationalising the evolution of the photoluminescence properties of lanthanide silicates across dimensionality.
© 2007 Elsevier B.V. All rights reserved.

*Keywords:* Layered silicates; Photoluminescence

## 1. Introduction

Layered [1] microporous silicates are host-guest systems suitable for engineering multifunctional materials with tunable properties [2,3]. In particular, it has been shown that solids combining the properties of layered silicates (intercalation chemistry) or zeolites (such as ion-exchange and molecular sieving) and photoluminescence may be obtained by inserting $Ln^{3+}$ cations in the frameworks, layers, micropores and interlayer spaces [4]. While research into zeolites made photoluminescent by Ln-doping via ion-exchange is not new, the preparation of layered and zeolite-type stoichiometric Ln silicates is an emerging field [5].

Recently, we have reported the synthesis, structure and photoluminescence properties of mixed layered Ln silicates $K_3[M_{1-a}Ln_aSi_3O_8(OH)_2]$, $M = Y^{3+}$, $Tb^{3+}$, $Ln = Eu^{3+}$, $Er^{3+}$, $Tb^{3+}$ and $Gd^{3+}$ [1] and $K_3[M_{1-a}Ce_aSi_3O_8(OH)_2]$, $M = Y^{3+}$, $Tb^{3+}$, $a \ll 1$ [6], named AV-22 materials. Calcining these layered silicates yields the small-pore ($K_3LnSi_3O_9$), $Ln = Y$, Eu, Tb, Er solids, named AV-23 [7]. Building upon this work, we now wish to report on the related $K_3[Y_{1-a}Er_aSi_3O_8(OH)_2]$ system and compare the photoluminescence features of as-prepared Y/Er-AV-22 and calcined Y/Er-AV-23.

## 2. Experimental methods

### 2.1. Synthesis

The syntheses of precursor layered AV-22 silicates were carried out in Teflon-lined autoclaves (volume 37 cm$^3$, filling rate 0.62), under static hydrothermal conditions, in ovens preheated at 230 °C. The autoclaves were removed and quenched in cold water after an appropriate time. The obtained microcrystalline powders were filtered, washed at room temperature with distilled water, and dried at 100 °C.

#### 2.1.1. Typical Y-AV-22, Er-AV-22 and mixed Y, Er AV-22 synthesis

An alkaline solution was made by mixing 4.45 g sodium silicate solution (27% m/m SiO$_2$, 8% m/m Na$_2$O, Merck), 15.97 g H$_2$O, 7.69 g KOH (Merck). An amount of 1.69 g of YCl$_3$·6H$_2$O (Aldrich) was added to this solution, and the mixture was stirred thoroughly. The gel, with composition 0.28 Na$_2$O:3.42 K$_2$O:1.0 SiO$_2$:0.14 Y$_2$O$_3$:44 H$_2$O was autoclaved under autogeneous pressure for 7 days at 230 °C. Er lamellar silicates were synthesised with substitution of YCl$_3$·6H$_2$O by ErCl$_3$·6H$_2$O (Aldrich). $K_3(Y_{1-a}Er_aSi_3O_9)$, $a = 0.005$–1, samples were synthesised by introducing the desired Er$^{3+}$ and Y$^{3+}$ contents in the initial gel.

### 2.2. Characterisation

SEM images were recorded on a Hitachi S-4100 microscope. EDS was carried out using an EDS Römteck System with polymeric window attached to the scanning electron microscope. All samples purity was verified by powder XRD (X'Pert MPD Philips diffractometer, Cu K( X-radiation). TGA curves were measured on a Labsys$^{TM}$ TG-DTA1600°Crod, from TA instruments, under nitrogen, using a 10 °C/min rate.

Raman spectra were recorded on a FT-Raman Bruker spectrometer, model RSF 100, at room temperature. The excitation source was a YAG:Nd laser ($\lambda_{Exc.} = 1064$ nm) (excitation power 400 mW for Y/Er-AV-22 and 50 mW for Y/Er-AV-23). The energy values from Raman shift (cm$^{-1}$), $E_R$, were converted
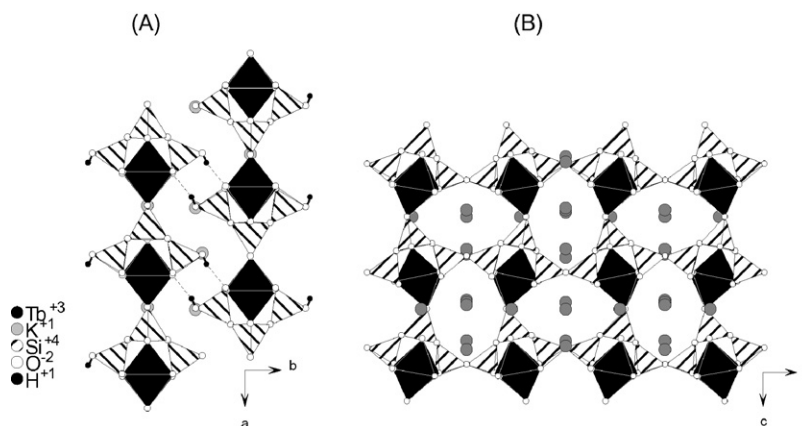
Fig. 1. (A) Polyhedral representation of AV-22 crystal packing viewed along gthe *c*-axis. Dashed lines depict O–H···O bonds. (B) Polyhedral representation of the crystal packing in AV-23, viewed along the *b*-axis.

into emission energy ($cm^{-1}$), $E_E$, using the expression: $E_E = E_{Laser} - E_R$, where $E_{Laser} = 9398.5 \, cm^{-1}$.

## 3. Results and discussion

To aid the discussion of the photoluminescence results, the structure of AV-22 and AV-23 materials are briefly described (Fig. 1). Ln-AV-22 contains a single crystallographic $Ln^{3+}$ centre (a slightly distorted $LnO_6$ octahedron) coordinated to six $SiO_4$ tetrahedra. The crystal structure may be described as the parallel packing in an [ABAB···] fashion along the *b*-axis direction of $[LnSi_3O_8(OH)_2]_n^{3n-}$ anionic layers (two per *b*-axis), which are further interconnected through strong O–H···O hydrogen bonds between neighboring Si–OH groups (Fig. 1A) [1]. The AV-22 dehydration causes the disordered condensation of adjacent two-dimensional $[LnSi_3O_8(OH)_2]_n^{3n-}$ nets yielding AV-23. The Ln-AV-23 structure contains a single crystallographically independent $Ln^{3+}$ metal centre coordinated to six {$SiO_4$} tetrahedra in a distorted octahedral geometry. Individual {$LnO_6$} octahe-

dra are isolated from each other by wollastonite-type siliceous chains, $(Si_6O_{17})_n^{10n-}$, running parallel to the *a*-axis of the unit cell (Fig. 1B). The shortest Ln···Ln internuclear distance for Ln-AV-22 and Ln-AV-23 are very similar 5.9072(12) Å [symmetry code: (i) *x*, *y*, *z* + 1] and 5.909(1) Å [symmetry code: (i) *x*, 1 + *y*, *z*]. The anionic $[LnSi_3O_9]_n^{3n-}$ framework is characterised by a three-dimensional channel system, filled with highly disordered $K^+$ cations, with the main tunnels running parallel to [1 0 0] and [0 1 0]. The former are evocative of the distorted seven-membered pores of the anionic $[LnSi_3O_8(OH)_2]_n^{3n-}$ (Ln-AV-22) layers which, upon layer condensation, align with the *a*-axis forming channels. The latter, more regular channels, are formed by eight-membered elliptical rings with a cross-section of *ca.* 2.0 Å × 4.0 Å (Fig. 1B).

FT-Raman spectra were recorded in order to quantitatively study the photoluminescence intensity as a function of the $Er^{3+}$ content in the Y/Er-AV-22 system $K_3[Y_{1-a}Er_aSi_3O_8(OH)_2]$, $a = 0.005–1$ (Fig. 2). As expected, the vibronic transitions appear in the Raman shift range 50–1200 $cm^{-1}$, while the intra $4f^{11}$
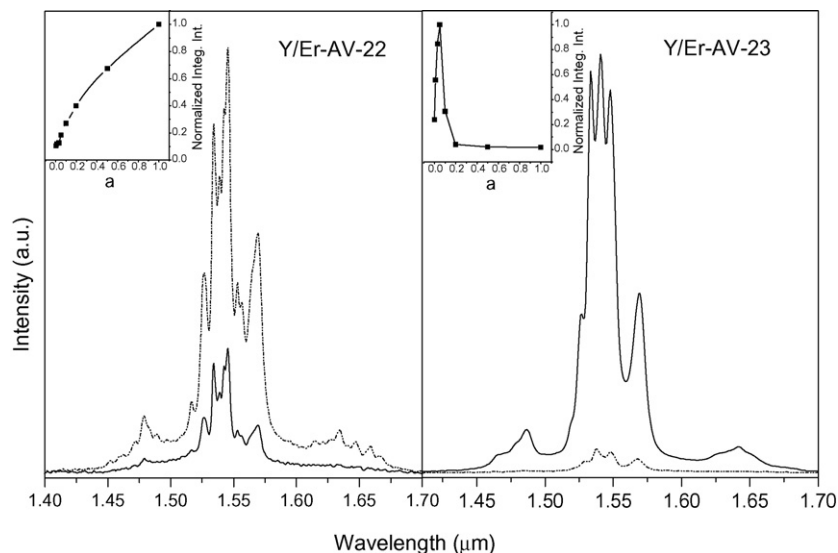


Fig. 2. FT-Raman spectra of Y/Er-AV-22 and Y/Er-AV-23: *a* = 0.1 (solid line) and *a* = 1.0 (dashed line). The insets depict the normalized integrated intensity of the 1.54 μm photoluminescence as a function of the $Er^{3+}$ content for the samples with *a* in the range 0.005–1.

electronic transitions are detected at 3500–2500 cm$^{-1}$. The emission lines are assigned to the intra $4f^{11}$ transitions between the $^4I_{13/2}$ and $^4I_{15/2}$ levels of the ground multiplet of $Er^{3+}$. Provided the intensities of the vibrational spectra of the different samples in the series are similar, the variation of the photoluminescence intensity as a function of the $Er^{3+}$ content may be estimated directly from the intensity of the strongest electronic line (1.54 µm) in the 3500–2500 cm$^{-1}$ (insets in Fig. 2). While in Y/Er-AV-22 the $^4I_{13/2} \rightarrow {}^4I_{15/2}$ emission integrated area increases with increasing $Er^{3+}$ content, due to the larger number of optically-active centres, in Y/Er-AV-23 the corresponding integrated area increases with increasing $Er^{3+}$ content, from 0.005 to 0.05, and decreases above this concentration. In Y/Er-AV-22 samples the photoluminescence is essentially quenched by the presence of OH vibrations, while in the Y/Er-AV-23 silicates (no OH groups present) the emission quenching is dominated by the $Er^{3+}$–$Er^{3+}$ interactions, probably mediated by the cross-relaxation mechanism. We note that the $Er^{3+}$–$Er^{3+}$ distances are similar in both silicates. Moreover, keeping constant the detection conditions and $Er^{3+}$ concentration, the emission intensity of the calcined material is much larger than the intensity of the precursor.

## 4. Conclusions

The synthesis and photoluminescence properties of new layered rare-earth silicates $K_3[Y_{1-a}Er_aSi_3O_8(OH)_2]$, $a = 0.005–1$ (Y/Er-AV-22) and calcined Y/Er-AV-23 have been reported. The calcination process increases the intensity of the $Er^{3+}$ emission (essentially due to the removing of OH groups) and the importance of the $Er^{3+}$–$Er^{3+}$ interactions as a quenching emission channel.

## References

[1] D. Ananias, M. Kostova, F.A. Paz, A. Ferreira, L.D. Carlos, J. Klinowski, J. Rocha, J. Am. Chem. Soc. 126 (2004) 10410.
[2] D. Ananias, A. Ferreira, J. Rocha, P. Ferreira, J.P. Rainho, C. Morais, L.D. Carlos, J. Am. Chem. Soc. 123 (2001) 5735.
[3] J. Rocha, P. Ferreira, L.D. Carlos, A. Ferreira, Angew. Chem. Int. Ed. 39 (2000) 3276.
[4] J. Rocha, L.D. Carlos, A. Ferreira, J. Rainho, D. Ananias, Z. Lin. Mater. Sci. Forum 527 (2004) 455.
[5] J. Rocha, L.D. Carlos, Curr. Opin. Solid State Mater. Sci. 7 (2003) 199.
[6] M.H. Kostova, R.A. Ferreira, D. Ananias, L.D. Carlos, J.C. Rocha, J. Phys. Chem. B 110 (2006) 15312.
[7] M.H. Kostova, D. Ananias, F.A. Paz, A. Ferreira, J. Rocha, L.D. Carlos, J. Phys. Chem. B 111 (2007) 3576.